3D Reconstruction of Retinal Blood Vessels from Two Views

Martinez-Perez, M.E.
IIMAS, UNAM, Mexico.
elena@leibniz.iimas.unam.mx

Espinosa-Romero, A.
FM, UADY, Mexico.
eromero@tunku.uady.mx

Abstract

A 3D reconstruction of retinal blood vessel trees using two views of fundus images is presented. The problem addresses: 1) The recovery of camera-eye model parameters by an self-calibration method. The camera parameters are found via the solution of simplified Kruppa equations, based on correspondences captured by hand from four different views. 2) The extraction of blood vessels and skeletons from two fundus images. 3) The match of correspondence points of the two skeleton trees. The trees are previously labelled during the analysis of 2D binary images. 4) The lineal triangulation of matched correspondence points, and the surface modeling using diameter measurements extracted from the 2D binary images. Examples from 3D skeletons and tree surfaces reconstructed models are shown.

1. Introduction

Quantitative assessment of retinal vasculature provides useful clinical information to assist in the diagnosis of various diseases. The detection and measurement of retinal vasculature can be used to quantify the severity of disease and the progression of therapy. Retinal blood vessel tree geometry, topology and vessel tracking have been widely studied by means of digital image processing mainly using retinal images which are also known as fundus images [7, 8]. However, the majority of these works have been carried out in 2D fundus images, like those shown in Figure 1 (a,c). A first effort to obtain a 3D view of fundus images has been developed by Deguchi, *et.al.* [2, 3]. Their work is focused on the reconstruction and display of 3D fundus patterns using branching vessel points correspondences between images for two and multiple views. As far as we are aware it has not been an attempt on extract and represent 3D models of retinal blood vessel trees particularly.

Photogrammetry analysis of features in human ocular fundus images is affected by various sources of error, for example aberrations of the fundus camera and the eye optics. The magnification in a fundus image is equal to the focal length of the fundus camera divided by the focal length of the eye. This formula can only occur under different ametropic conditions and changes in the camera position with respect to the subject's eye. These differences in magnification between one fundus image and another has been pointed out by Arnold *et. al.* [1]. As a result, it is not possible to make a direct comparisons between measurements on different subjects. Another type of distortion arises from projecting the near spherical shape of the fundus onto a planar imaging device. Consequently, 3D reconstruction of retinal blood vessel trees up to a metric projection is a great challenge.

In this paper we present a first approximation to the solution of this problem. 3D reconstruction of fundus vasculature conveys the following questions: 1) the estimation of the intrinsic camera parameters (calibration matrix K) for each "fundus camera-eye ball" system, 2) the extraction of blood vessel trees from 2D fundus images, 3) the match of the correspondences of vessel skeleton tree points between images, 4) the computation of the fundamental matrix (F) from the correspondences, 5) the computation the camera projection matrices (P, P') from fundamental matrix, 6) for each correspondence point, the computation of a point in the space via triangulation and finally, 7) the construction of a 3D model of the blood vessel tree surface.

The rest of the paper is organised as follows: section 2 describes the techniques that we follow to estimate K and F matrices; section 3(a,c) deals with blood vessel extraction and analysis of binary images from 2D fundus images. Section 4 details the computation of the projection matrices and the triangulation procedure to get 3D views of vessel tree skeletons, section 5 depicts the first approach to surface reconstruction, and finally sections 6 and 7 present some experimental results and conclusions.

2. Camera calibration

The calibration task we are dealing with, is particularly difficult since we ignore the intrinsic and extrinsic parameters of the fundus camera used to capture the images as well as those parameters of the optical system formed by the cornea, lens and vitreous humor of the eye-ball being examined. Thus, we need to use a self-calibration technique which uses a number of specific correspondences of branching and crossing blood vessel points. These points are taken from a set of retinal images captured from different views

of the same eye-ball.

The method we applied to camera self-calibration is based on the work reported by [6] which employs a simplification of the Kruppa equations. The method relies solely on the singular value decomposition (SVD) of the fundamental matrix that reduces the number of equations to be solved. It also avoids to recover noise-sensitive quantities such as epipoles, since its accurate estimation is difficult in the presence of noise and/or degenerate motions. In the next sections we will outline the algorithm (for details see [6]).

2.1. Compute the calibration matrix (K)

Kruppa equations can be considered as an epipolar matching constraint for the projections of quadratics or conics [4]. The image conics are identical when the images are captured with a camera with fixed intrinsic parameters, which is the case of any pair of views taken with the fundus camera. Let ω be the projection of the absolute conic. The matching constraint can be expressed in the following form:

$$F\omega^* F^T = [e']_\times \omega^* [e']_\times \tag{1}$$

where F is the fundamental matrix of the two views, e' is the second epipole. The equality is up to scale ($\omega^* = \omega^{-1}$, dual image of the absolute conic) and $[e']_\times$ is the skew-symmetric matrix associated with the cross-product of e'. Expression 1 is called the *Kruppa equations*.

Using singular value decomposition (SVD) of matrix $F = UDV^T$, expression 1 is equivalent to:

$$\frac{u_2^T \omega^* u_2}{r^2 v_1^T \omega^* v_1} = -\frac{u_1^T \omega^* u_2}{rs v_1^T \omega^* v_2} = \frac{u_1^T \omega^* u_1}{s v_2^T \omega^* v_2} \tag{2}$$

where r, s are the eigenvalues of the matrix FF^T; u_1, u_2, u_3 are the column vectors of U; v_1, v_2, v_3 are the column vectors of V, and U, V are two orthogonal matrices. The aim is to find ω^*.

The camera calibration matrix, K, is a 3×3 matrix having the well-known form:

$$K = \begin{bmatrix} \alpha_u & -\alpha_u cot\theta & u_0 \\ 0 & \alpha_v / sin\theta & v_0 \\ 0 & 0 & 1 \end{bmatrix} \tag{3}$$

where α_u and α_v correspond to the focal distances in pixels along the axes of the image, θ is the angle between the two image axes and (u_0, v_0) are the coordinates of the principal point.

$$\omega^* = KK^T \tag{4}$$

therefore the matrix K is extracted from ω^* by computing K^T employing the Cholesky decomposition of ω^{-1}, then it is transposed and finally inverted to yield K.

We summarise the algorithm to find ω^* in two steps:

1. Finding initial solution. A good approximation for the initial solution is to assume that principal point coincides with the center of image and that skew angle θ is equal to $\frac{\pi}{2}$. The two focal lengths α_u, α_v, are initialised randomly. Assuming that we have M images, that have been acquired with constant camera intrinsic parameters, a total of $N \leq \frac{M(M-1)}{2}$ fundamental matrices can be defined.

2. Non-Linear Optimisation. Let $\pi_{ij}(S_F, \omega^*)$ denote the differences of ratios ij and $\sigma_{ij}^2(S_F, \omega^*)$ the variance from equation 2. Matrix ω^* is computed as the solution of the non-linear least squares problem:

$$\begin{aligned} \omega^* = \quad & argmin_{\tilde{\omega}^*} \sum_{i=1}^{N} \frac{\pi_{12}^2(S_{F_i}, \tilde{\omega}^*)}{\sigma_{\pi 12}^2(S_{F_i}, \tilde{\omega}^*)} + \frac{\pi_{13}^2(S_{F_i}, \tilde{\omega}^*)}{\sigma_{\pi 13}^2(S_{F_i}, \tilde{\omega}^*)} \\ & + \frac{\pi_{23}^2(S_{F_i}, \tilde{\omega}^*)}{\sigma_{\pi 23}^2(S_{F_i}, \tilde{\omega}^*)} \end{aligned} \tag{5}$$

where S_F is a vector form by parameters from the SVD of F. The minimization of equation 5 is done using classical Levenberg-Marquardt algorithm [10].

2.2. Compute the fundamental matrix (F)

The fundamental matrix is defined by the equation

$$x'^T F x = 0 \tag{6}$$

for any pair of matching points $x_i \leftrightarrow x_i'$. From a set of n point matches, we obtain a set of linear equations as:

$$Af = 0 \tag{7}$$

where A is composed by the matches $x_i \leftrightarrow x_i'$. The method to find F is based on the normalised 8-point algorithm [4] that can be summarised as follows:

1. Normalisation: Transform the image coordinates according to $\hat{x}_i = Tx_i$ and $\hat{x}_i' = T'x_i'$, where T and T' are normalised transformations consisting of a translation and scaling.

To find the fundamental matrix $\hat{F}'$ of matches $\hat{x}_i \leftrightarrow \hat{x}_i'$:

2. Linear solution: Determine $\hat{F}$ as the solution of equation 7 from the SVD of $\hat{A} = UDV^T$.

3. Constraint enforcement: Force matrix $\hat{F}$ to have rank 2 by replacing $\hat{F}$ by $\hat{F}'$ such that $det\hat{F}' = 0$.

4. Denormalisation: Set $F = T'^T \hat{F}' T$. Matrix F is the fundamental matrix corresponding to the original data $x_i \leftrightarrow x_i'$.

3. Blood vessel extraction

Blood vessels are segmented using a previously described algorithm based on multi-scale analysis [7]. Two geometrical features based upon the first and the second derivative of the intensity image, maximum gradient and principal curvature, are obtained at different scales by means of Gaussian derivative operators. A multiple pass region growing procedure is used which progressively segments the blood vessels using the feature information together with spatial information about the 8-neighbouring pixels. Figure 1(a) and (c) shows two scanned negative of a retinal photographs and

Figure 1(b) and (d) their segmented binary images respectively, where the optic disc region is on the top centre, vessels are tracked from this area outwards.

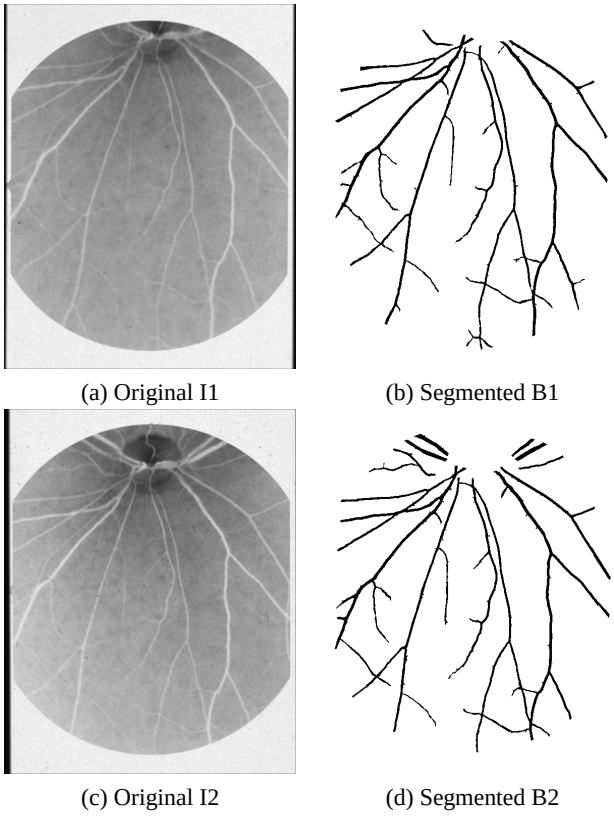

(a) Original I1 (b) Segmented B1

(c) Original I2 (d) Segmented B2

Figure 1: (a) and (c) two views, from the same eye-ball, of scanned negatives and (b) and (d) their respective segmented images.

3.1. Analysis of binary images

A semi-automatic method to measure and quantify geometrical and topological properties of continuous vascular trees in clinical fundus images was developed on a previous work [8]. Measurements are made from segmented binary images. The skeletons of the segmented trees are produced by a thinning technique, branching and crossing points are identified and segments of the trees are labelled and stored as a chain code. The operator selects the tree to be measured and decides if it is an arterial or venous tree. An automatic process then measures the lengths, areas and angles of the individual segments of the tree. Geometrical data such as diameter, length, branching angle, and the connectivity information between segments from continuous retinal vessel trees are tabulated. A number of geometrical properties and topological indices are derived. Figure 2 shows three different vessel trees extracted from Figure 1(b). Note that in these images (Figure 2) only vessel segments are extracted,

(a) (b) (c)

Figure 2: (a)-(c) Three different vessel trees extracted from binary image shown in Figure 1(b).

branching areas are ignore. From each tree, an ASCII table of measurements is generated.

4. 3D skeleton reconstruction

Suppose that a set of image correspondences $x_i \leftrightarrow x'_i$ are given, such as the skeleton points. It is assumed that these correspondences come from a set of 3D points X_i, which are unknown. The reconstruction task is to find the camera projection matrices P and P', as well as the 3D points X_i such that

$$\begin{aligned} x_i &= PX_i \\ x'_i &= P'X_i \quad \text{for all } i \end{aligned} \tag{8}$$

The reconstruction process consist on: 1) compute the fundamental matrix F from the correspondences, 2) compute the camera projection matrices, P and P', from fundamental matrix, and 3) for each point correspondence $x_i \leftrightarrow x'_i$ compute the point in the space that projects these two image points.

4.1. Compute the camera projection matrices.

Consider a camera matrix decomposed as $P = K[R|t]$, where R is the rotation matrix and t is the translation vector. The essential matrix (E) is the fundamental matrix corresponding to the pair of normalised cameras. The relationship between the fundamental matrix and essential matrix is given by:

$$E = K'^T F K \tag{9}$$

The camera projection matrices may be retrieved from E up to scale and a four-fold ambiguity. Thus, we can follow the next 3 step algorithm [5]:

1. Assume that the reference frame is centered in the first camera matrix as $P = [I|0]$ in order to compute the second camera matrix P'.

2. Factor E into the product SR of a skew-symmetric matrix and a rotation matrix, by the SVD of E.

3. Since $St = 0$, it follows that $t = U(0, 0, 1)^T = u_3$. However, the sign of E and consequently t cannot be

determined. Thus, for a given essential matrix there are four possible choices of the camera P' based on two possible choices of R and two possible signs of t. Testing with a single point to determine if it is in front of both cameras is sufficient to decide between the four different solutions for the camera matrix P'.

4.2. Compute the 3D points by triangulation.

The 3D points X_i are calculated by performing a linear triangulation using the inhomogeneous method [4]. Equations 8 can be combined into a form $AX = 0$, which is an equation linear in X, with

$$A = \begin{bmatrix} xp^{3T} - p^{1T} \\ yp^{3T} - p^{2T} \\ x'p'^{3T} - p'^{1T} \\ y'p'^{3T} - p'^{2T} \end{bmatrix} \quad (10)$$

where p^{iT} are the rows of P. Setting $X = (X, Y, Z, 1)^T$, the solution of $AX = 0$, can be found by a least-squares method.

5. Surface modelling.

Since the 3D reconstruction algorithm described in section 4 is applied only to the skeleton points of each blood vessel tree, we did not recover 3D information from the actual shape of its surface. We considered a fair assumption to describe the blood vessel segment cross-section as a circle in order to generate a 3D surface. Each blood vessel segment was modelled by a generalised cylinder [9] which axis is the 3D skeleton estimated earlier. The radius of each circular cross-section is kept constant for each vessel segment, and it is calculated from measures obtained from the 2D fundus images [8]. The cylinders are scaled using the camera internal parameters from matrix K.

6. Experimental results

A set of fundus images were taken from the same subject and same eye ball. Retinal photographs were taken using a fundal camera with 30° field of view (Kowa FX-50R, Kowa, Tokyo, Japan). Ilford FP4 (125 ASA) photographic film was used. Photographic negatives were digitised using a Nikon 35*mm* film scanner (LS-100, Nikon, Tokyo, Japan). Digitised images were 720×577 pixels in size. For the purpose of these experiments, 4 different views were taken for the calibration process and one different pair for the reconstruction example from this data set.

6.1. Camera calibration matrix (K)

Four different views of the fundus negative images were chosen for calibration purposes. 16 matched points were selected by hand in each of the four images. Branching points, vessel crossing points and points around the optic disc were selected as references. Figure 3 shows these four images with the points selected marked on white.

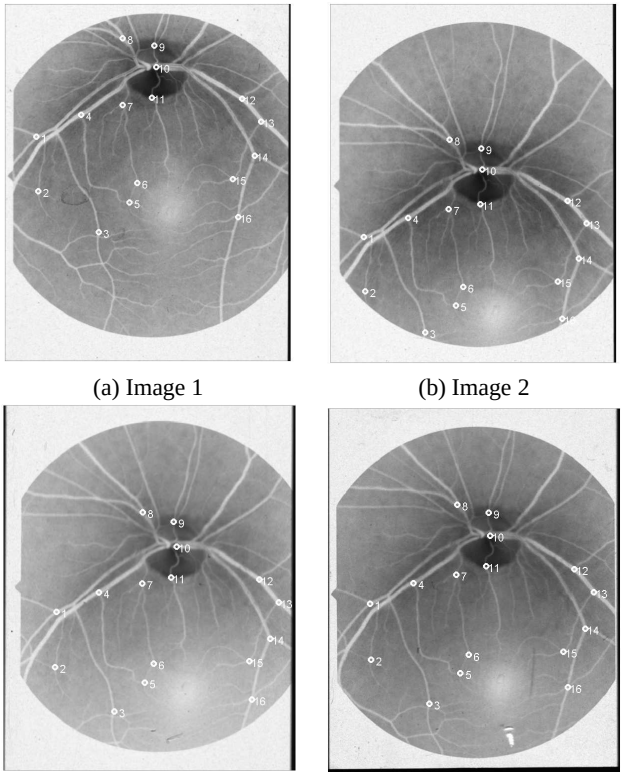

(a) Image 1 (b) Image 2

(c) Image 3 (d) Image 4

Figure 3: (a)-(d) Fundus negative images chosen for calibration purposes. The 16 hand selected matched points are marked in white.

Since we have 4 images, that have been acquired with constant camera intrinsic parameters a total of 6 fundamental matrices can be defined. We assumed the initialisation parameters described in section 2.1. Fundamental matrices for each par of images are computed using the 8-points algorithm described in section 2.2. From equations 4 and 5 we obtained the calibration matrix equal to:

$$K = \begin{bmatrix} 424.8281 & 1.0000 & 470.9406 \\ 0 & 969.9713 & 128.0000 \\ 0 & 0 & 1.0000 \end{bmatrix}$$

6.2. 3D skeleton reconstruction

One pair of images was selected and segmented from our data set of photographs as shown in Figure 1 (a,c) [7]. Skeletons of separated blood vessel trees, as those shown in Figure 2, are marked and measured. Measurements are kept in an ASCII table per tree [8].

Since continuous blood vessel tree skeletons are marked they can be tracked along the tree. Using these tables, the

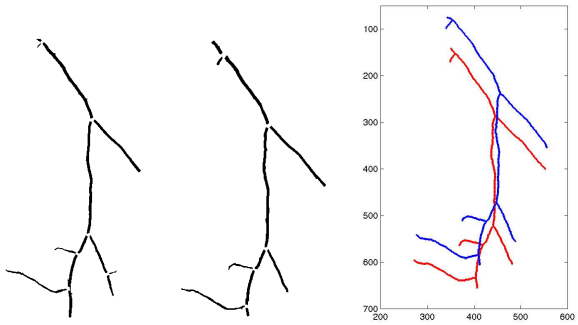

(a) T2, I1 (b) T2, I2 (c) T2, match

Figure 4: (a) Tree #2 from image I1, (b) Tree # 2 from image I2, and (c) the matched tree skeletons.

correspondences ($x_i \leftrightarrow x_i'$) of a continuous tree skeletons from the two pair of images are extracted automatically. Figures 4(a) and (b) show the same tree extracted from images Figure 1(b) and (d) respectively. Figure 4(c) shows the corresponding matched tree skeletons. Note that a small branch at the bottom-right of the tree shown in Figure 4(a) is missing in the image of the same eye shown in Figure 4(b). This small branch is of course automatically discarded in the correspondences like it is shown in Figure 4(c).

A set of correspondences $x_i \leftrightarrow x_i'$ of only one tree is needed in order to compute the two projection matrices P and P', as described in section 4.1, with the use of the camera calibration matrix K calculated in section 6.1.

Once the projection matrices are obtained, the triangulation of the rest of correspondences per each skeleton tree extracted from the pair of images is done. A total of 5 trees were reconstructed for this example. Correspondences were interpolated using splines in order to obtain a smoother version of the reconstructed skeletons. Figure 5 shows different 3D views of the blood vessel skeletons extracted and plotted on the same coordinate system.

Note that optic disc is at the bottom of the coordinate system therefore tree roots are in that area. Figure 5(a) shows the curvature of the eye ball, this view corresponds to a 30° filed of view of the fundus camera. The other three views (b)-(d) are just rotated versions of the former.

6.3. Surface visualisation

Using the surface model described in section 5 and based on the 3D skeleton points and vessel segment diameter, the surface of each vessel segment is generated. Each tree is visualised using Geomview[1], a 3D viewing program. Each tree is built as a set of disconnected segments such as those shown in Figure 2(a), each of them with a defined spatial position and orientation.

[1] `http://www.geomview.org/`

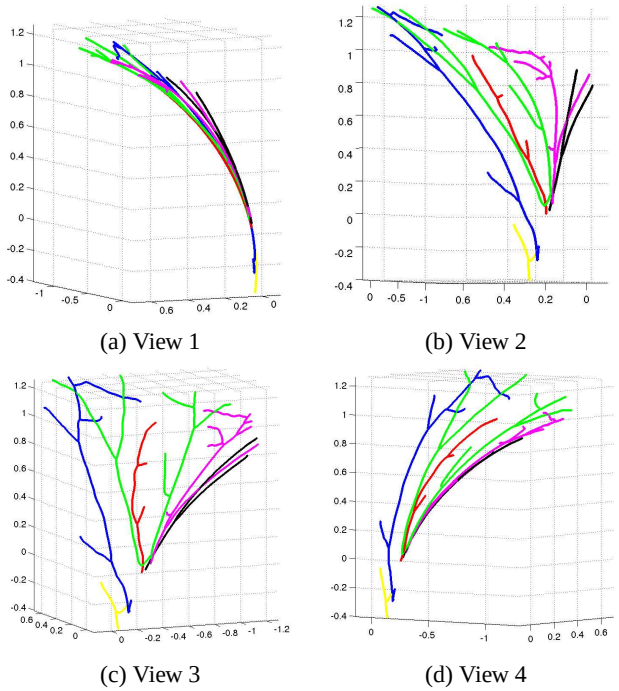

(a) View 1 (b) View 2

(c) View 3 (d) View 4

Figure 5: (a)-(d) Four different 3D views of skeleton trees reconstruction, extracted from pair of images shown in Figure 1.

Each vessel segment surface is described by a mesh of square patches wrapped in one direction so that it forms a cylinder. The mesh vertices for each segment are calculated as follows: for each 3D skeleton point, the set that describes the generalised cylinder axis, a polygon or cross–section is considered. Each polygon is centered in the 3D axis position in space, and its orientation is set so that the vector normal to the polygon center is tangent to the skeleton axis at that point. The coordinates of the polygon vertices are used as the mesh vertices. Each vertex is connected to the two neighbouring vertices in the same cross–section and to the corresponding vertices in the neighbouring cross-sections. The vertices of the cross-section at the extreme points of each segment are only connected to one neighbouring cross-section. Four 3D views of different vessel trees are shown in Figure 6.

Figure 6(a) corresponds to the surface reconstruction of the tree shown in Figure 4. Figure 6(b) is the same tree from (a) but rotated to show the eye ball curvature. Figures 6(c) and (d) show the examples of two other reconstructed trees. Note that in this case optic disc is at the top of the coordinate system, and blood vessel segments coming from that area are wider than those from the tips of the tree.

7. Conclusions

We have presented a 3D retinal blood vessel tree model, reconstructed from two different views of 2D fundus images through: self-calibration procedure, 3D projection, triangu-

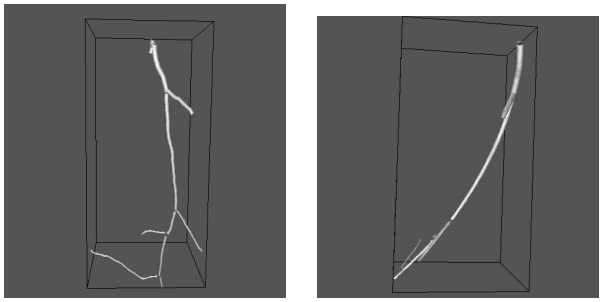

(a) Tree 2 (b) Tree 2

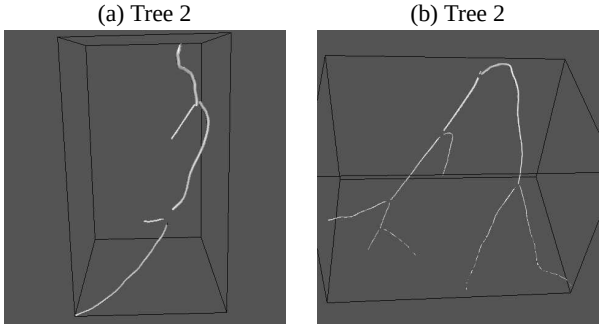

(c) Tree 4 (d) Tree 4

Figure 6: (a)-(d) Four different 3D views of blood vessel trees, extracted from pair of images shown in Figure 1. Diameter measure of each vessel segment is obtained from the 2D binary image.

lation and surface meshing.

One of the main differences that we found from Deguchi, *et.al.* [2, 3] work compare with ours, is that they do not used self-calibration procedure, instead they employ two parallel planes in front of the fundus camera and use a transparent acrylic plate with a grid in order to calibrate the camera. Along with it, they project the correspondences and fundus pattern into a spherical surface which means that even a crossing point belongs to the same surface. It can be seen from Figure 5(a) that all vessel trees follow the same eyeball curvature but do not belong exactly to the same spherical surface, which seems more realistic. Finally, we only reconstruct blood vessel trees rather than fundus patterns.

There are various questions that still have to be addressed in order to use this model for mensurable applications. First of all the selection of the 16 correspondence points used in the calibration process can be calculated automatically; at the present we can detect them automatically but a registration method have to be implemented [4]. Radial distortions are not taken into account. Since trees are extracted by individual vessel segments separately, branching regions are not considered in the mesh of the current model. Also it is necessary to perform a full error analysis of the geometric methods described in this article in order to evaluate the robustness of the proposed approach; this includes a validation of the self–calibration method and the factorization of the essential matrix. Nevertheless our results suggest that, after clearing up these issues, the 3D model obtained could be used for realistic applications.

Representation of vascular trees with 3D models could have many advantages on opthalmology: it could give a more realistic view for physicians for clinic and education purposes, it could permit to extend all geometrical and topological properties already measured in 2D images [8] to a 3D model, and it could allow to have a 3D geometry which could be used for blood flow simulations.

Acknowledgement

Thanks to the Dept. of Clinical Pharmacology, Imperial College of Science, Technology & Medicine for the clinical images.

References

[1] J. Arnold, J. Gates, and K. Taylor. Possible errors in the measurement of retinal lesions. *Invest. Ophthalmol. & Vis. Sci.*, 34:2576–2580, July 1993.

[2] K. Deguchi, D. Kawamata, K. Mizutani, H. Hontani, and K. Wakabayashi. 3d fundus shape reconstruccion and display from stereo fundus images. *IEICE Trans. Inf. & Syst.*, E83-D(7), July 2000.

[3] K. Deguchi, J. Noami, and H. Hontani. 3d fundus pattern reconstruction and display from multiple fundus images. In *Proceedings. 15th International Conference on Pattern Recognition*, volume 4, pages 94 – 97, September 2000.

[4] R. Hartley and A. Zisserman. *Multiple View Geometry in computer vision*. Cambridge Uiversity Press, 2000.

[5] R. I. Hartley. Estimation of relative camera positions for incalibrated cameras. In *Proceedings of the 2nd European Conference on Computer Vision*, pages 579 – 587, May 1992.

[6] M. I. A. Lourakis and R. Deriche. Camera self-calibration using the singular value decomposition of the fundamental matrix: from point correspondences to 3d measurements. Technical Report INRIA 3748, Intitut National de Recherche en Informatique et en Automatique, August 1999.

[7] M. E. Martinez-Perez, A. D. Hughes, A. V. Stanton, S. A. Thom, A. A. Bharath, and K. H. Parker. Retinal blood vessel segmentation by means of scale-space analysis and region growing. In C. Taylor and A. Colchester, editors, *MICCAI-99*, volume 1679 of *Lectures Notes in Computer Science*, pages 90 – 97. Springer-Verlag, 1999.

[8] M. E. Martinez-Perez, A. D. Hughes, A. V. Stanton, S. A. Thom, N. Chapman, A. A. Bharath, and K. H. Parker. Retinal vascular tree morphology: A semi-automatic quantifi cation. *IEEE Transactions on Biomedical Engineering*, 49(8), August 2002.

[9] J. Ponce. Straight homogeneous generalized cylinders: Differential geometry and uniqueness results. *Inaternational Journal on Computer Vision*, 4(1):79–100, January 1990.

[10] W. Press, W. Vetterling, S. Teukolsky, and B. Flannery. *Numerical Recipes in C.* Cambridge Uiversity Press, 1995.